Laboratoire Kastler Brossel
Physique quantique et applications

le cnam

cnrs

SORBONNE UNIVERSITÉ
CRÉATEURS DE FUTURS DEPUIS 1257

ENS

Measuring the fine-structure constant to refine the Standard Model predictions

Saïda Guellati-Khélifa

The fine-structure constant

$$\alpha = \frac{e^2}{4\pi\epsilon_0\hbar c} \sim \frac{1}{137}$$

- Sommerfeld-Bohr: Naive model to explain the splitting of Balmer lines in hydrogen spectrum

Für das *eigentliche Balmersche Wasserstoffspektrum* $(E = e)$ kann man etwas kürzer schreiben:

(18a)
$$\begin{cases} \nu = \frac{m_0 c^2}{h}\left(1 + \frac{\alpha^2}{(n' + \sqrt{n^2 - \alpha^2})^2}\right)^{-1/2} \\ \qquad - \left(1 + \frac{\alpha^2}{(m' + \sqrt{m^2 - \alpha^2})^2}\right)^{-1/2} \end{cases}.$$

A. Sommerfeld, Annalen der Physik 51, 1-94, 125-167 (1916)

- First determination of the fine-structure constant $\frac{\sigma_\alpha}{\alpha} \simeq 0.004$

Test of Quantum electrodynamics and Standard model

α : coupling constant of electromagnetic interaction

Transition frequencies measurement

Muonium ground-state hyperfine splitting

$$\Delta\nu_{\mathrm{Mu}}(\mathrm{th}) = \Delta\nu_F \times \mathcal{F}(\alpha, m_\mathrm{e}/m_\mu)$$

$$\Delta\nu_F = \frac{16}{3} c R_\infty Z^3 \alpha^2 \frac{m_\mathrm{e}}{m_\mu}\left(1+\frac{m_\mathrm{e}}{m_\mu}\right)^{-3}$$

Anomalous Magnetic Moment of the Electron

$$a_\mathrm{e}(\mathrm{theo}) \equiv a_\mathrm{e}(\mathrm{exp})$$

Quantum Hall effect

$$R_\mathrm{K} = \frac{h}{e^2} = \frac{\mu_0 c}{2\alpha}$$

Recoil measurement

$$\alpha^2 = \frac{2R_\infty}{c}\frac{m_\mathrm{At}}{m_\mathrm{e}}\frac{h}{m_\mathrm{At}}$$

Paris, Berkeley

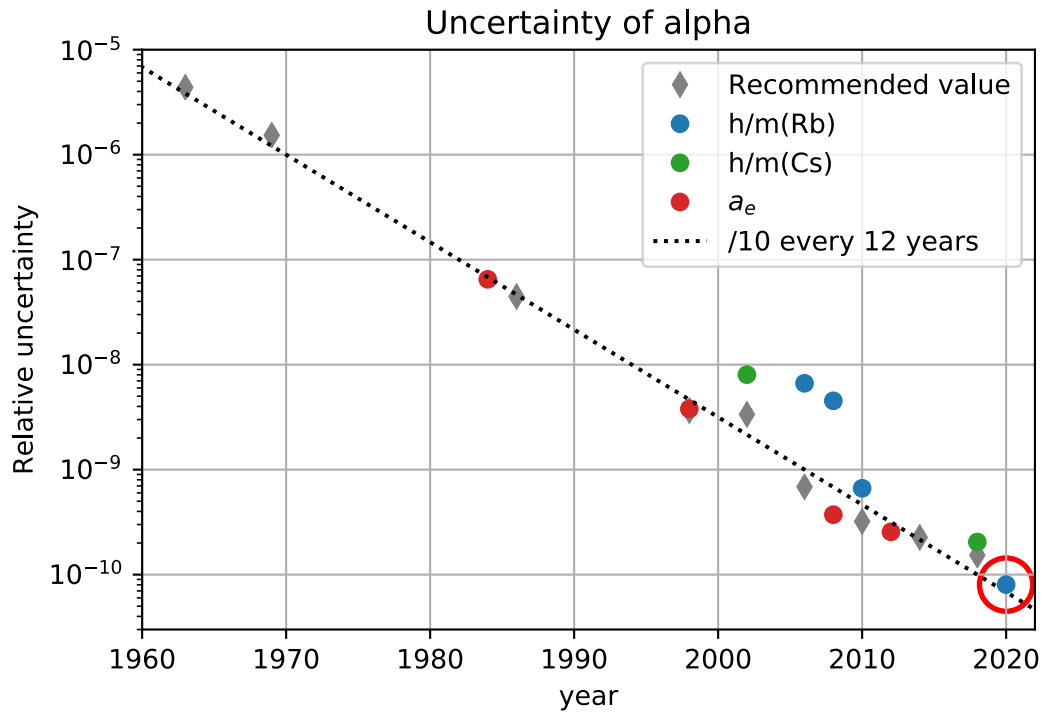

Physics beyond Standard Model ?

$$a_\mathrm{e}(\mathrm{theo}) - a_\mathrm{e}(\mathrm{exp}) \stackrel{?}{=} \delta a_\mathrm{e}(\mathrm{BSM})$$

Anomalous Magnetic Moment of the Electron

- Electron magnetic moment $\vec{\mu}_e = -g_e \mu_B \frac{\vec{S}}{\hbar}$ $\mu_B = \frac{e\hbar}{2m_e}$: Bohr magneton

- Vacuum fluctuations and polarization modify the interaction of the electron with the magnetic field,

$$\frac{g_e}{2} = 1 + a_e \simeq 1 + \frac{1}{2}\frac{\alpha}{\pi}$$

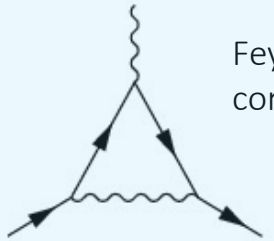

Feynman diagram for the one photon-loop correction for the free electron

Schwinger, Phys. Rev. 73, 416 (1948); Phys. Rev. 75, 898 (1949)

- Higher order corrections: perturbative series of $\alpha = 1/137.036 \approx 0.007$

J. Schwinger, R. Feynman, E. Stueckelberg, S. Tomonaga….

$$a_e(\text{QED}) = \underbrace{A_1}_{e,\gamma} + \underbrace{A_2(m_e/m_\mu)}_{e,\mu,\gamma} + \underbrace{A_2(m_e/m_\tau)}_{e,\tau,\gamma} + \underbrace{A_3(m_e/m_\mu, m_e/m_\tau)}_{e,\mu,\tau,\gamma}$$

$$A_i = A_i^{(2)}\left(\frac{\alpha}{\pi}\right) + A_i^{(4)}\left(\frac{\alpha}{\pi}\right)^2 + A_i^{(6)}\left(\frac{\alpha}{\pi}\right)^3 + A_i^{(8)}\left(\frac{\alpha}{\pi}\right)^4 + \cdots$$

QED contribution: 8th order term

- 891 Feynman diagrams contribute to 8th order $A_1^{(8)}$ term.

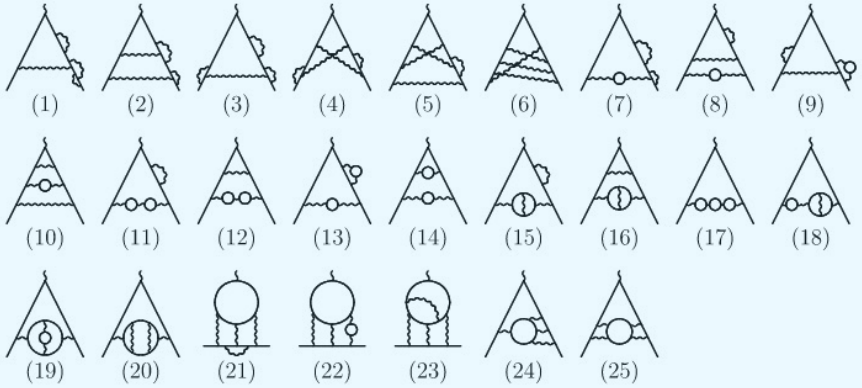

Standard model prediction of a_e

Coefficient $A_i^{(2n)}$	Value (Error)	References	
$A_1^{(2)}$	0.5	Schwinger 1948	
$A_1^{(4)}$	$-0.328\,478\,965\,579\,193\cdots$	Petermann 1957, Sommerfield 1958	
$A_2^{(4)}(m_e/m_\mu)$	$0.519\,738\,676\,(24)\times10^{-6}$	Elend 1966	
$A_2^{(4)}(m_e/m_\tau)$	$0.183\,790\,(25)\times10^{-8}$	Elend 1966	
$A_1^{(6)}$	$1.181\,241\,456\,587\cdots$	Laporta-Remiddi 1996, Kinoshita 1995	
$A_2^{(6)}(m_e/m_\mu)$	$-0.737\,394\,164\,(24)\times10^{-5}$	Samuel-Li, Laporta-Remiddi, Laporta	72 diagrams
$A_2^{(6)}(m_e/m_\tau)$	$-0.658\,273\,(79)\times10^{-7}$	Samuel-Li, Laporta-Remiddi, Laporta	
$A_3^{(6)}(m_e/m_\mu, m_e/m_\tau)$	$0.1909\,(1)\times10^{-12}$	Passera 2007	
$A_1^{(8)}$	$-1.912\,245\,764\cdots$	Laporta 2017, AHKN 2015	
$A_2^{(8)}(m_e/m_\mu)$	$0.916\,197\,070\,(37)\times10^{-3}$	Kurz et al 2014, AHKN 2012	
$A_2^{(8)}(m_e/m_\tau)$	$0.742\,92\,(12)\times10^{-5}$	Kurz et al 2014, AHKN 2012	891 diagrams
$A_3^{(8)}(m_e/m_\mu, m_e/m_\tau)$	$0.746\,87\,(28)\times10^{-6}$	Kurz et al 2014, AHKN 2012	
$A_1^{(10)}$	$6.737\,(159)$	AKN 2018,2019	
$A_2^{(10)}(m_e/m_\mu)$	$-0.003\,82\,(39)$	AHKN 2012,2015	
$A_2^{(10)}(m_e/m_\tau)$	$\mathcal{O}(10^{-5})$		12671 diagrams
$A_3^{(10)}(m_e/m_\mu, m_e/m_\tau)$	$\mathcal{O}(10^{-5})$		

- T. Aoyama, T. Kinoshita, M. Nio, Phys. Rev. D 2018, 97, 036001.
- S. Laporta, Phys. Lett. B 2017, 772, 232–238.
- T. Aoyama, T. Kinoshita and M. Nio, Atoms 2019, 7, 28
- R. Bouchendira et al., Phys. Rev. Lett. 2011, 106, 080801.
- R.H. Parker et al, Science 2018, 360, 191–195.

$$a_e(\text{theo}) = a_e(\text{QED}) + a_e(\text{Hadron}) + a_e(\text{Weak})$$

$$a_e(\text{theory} : \alpha(\text{Rb})) = 1159652182.037\ (720)\ (11)\ (12) \times 10^{-12}$$
$$a_e(\text{theory} : \alpha(\text{Cs})) = 1159652181.606\ (229)\ (11)\ (12) \times 10^{-12}$$

- (12): hadronic contribution
- (11): Numerical evaluation of the tenth-order QED
- (720) / (229): Fine-structure constant

Measurement of the anomalous magnetic moment of the electron

R. S. Van Dyck., P. B. Schwinberg and H. G. Dehmelt. Phys. Rev. D 34, 722 (1986) and Phys. Rev. Lett. 59, 26 (1987)

- Electron in a magnetic field

$$\frac{g_e}{2} = \left|\frac{\mu_e}{\mu_B}\right| = \frac{\nu_s}{\nu_c} = 1 + \frac{\nu_s - \nu_c}{\nu_c} = 1 + \frac{\nu_a}{\nu_c}$$

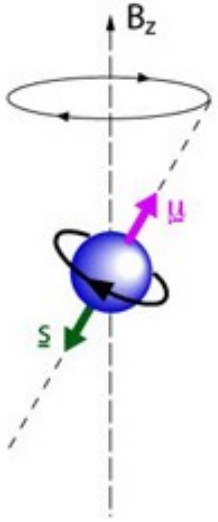

$$E_{n,m_s} = m_s h\nu_s + \left(n + \frac{1}{2}\right) h\nu_c$$

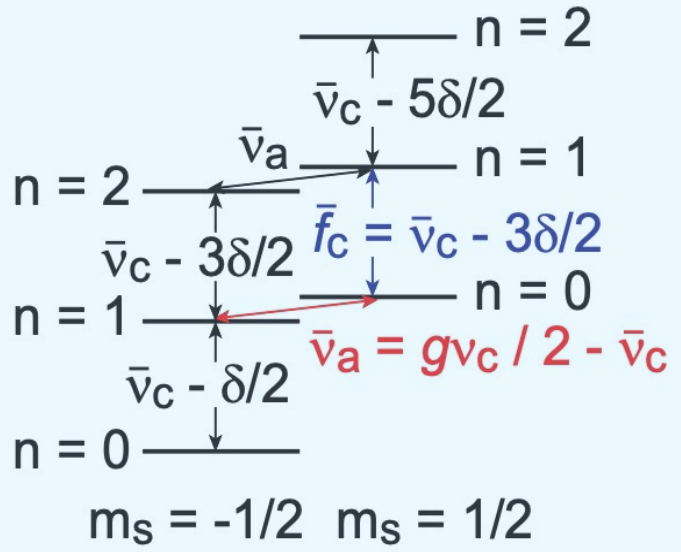

Advantages

- The magnetic field dependence drops out of the ratio.
- ν_c and ν_s differs by 10^{-3}, measuring frequencies to $10^{-10} \longrightarrow g_e$ to 10^{-13}

Measurement of the electron magnetic moment: Harvard experiment

- Electron in Penning trap + magnetic field

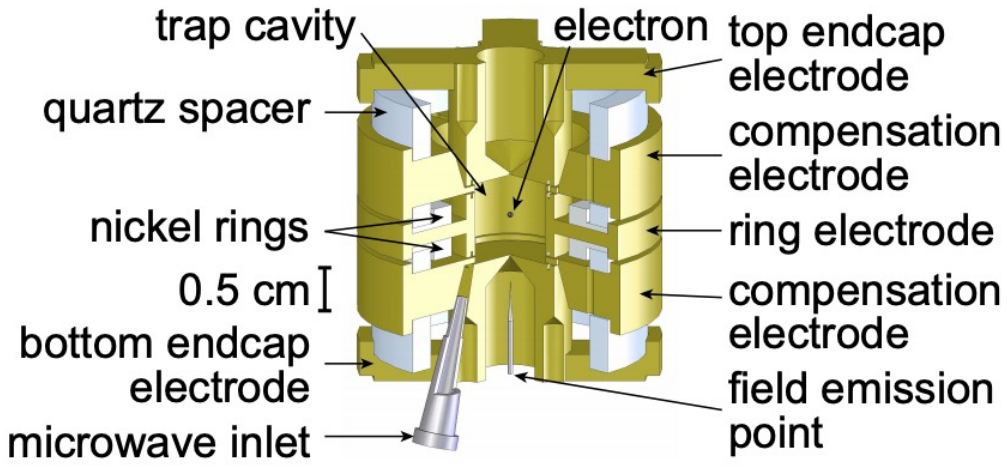

$$a_e(\mathrm{exp}) = \frac{g_e - 2}{2} = 0.00115965218073\ (28)\ [0.28\ \mathrm{ppt}]$$

Hanneke, D.; Fogwell, S.; Gabrielse, G. Phys. Rev. Lett. 2008, 100, 120801.

Quantum-jump spectroscopy

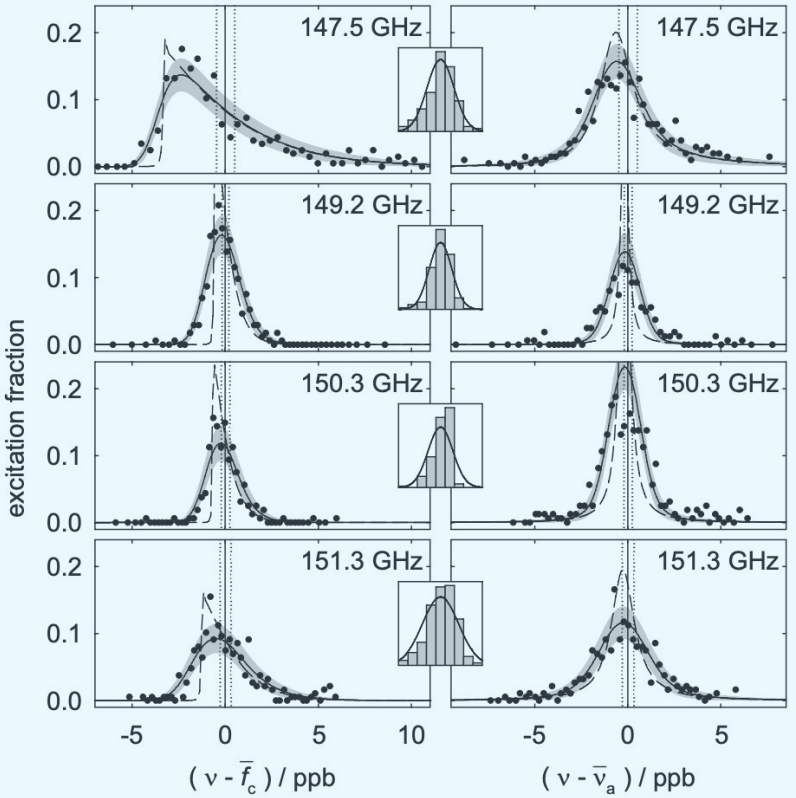

- 10 times improved accuracy is expected
  - New experimental setup (better control of the electron motion, reduction of magnetic field gradient)
  - The spin and cyclotron transition frequencies measured nearly simultaneously

X. Fan and G. Gabrielse, Phys. Rev. A 103, 022824 (2021)

The ratio h/m and the fine-structure constant

1928, Dirac equation

- Energy levels of hydrogen atom: $$E(n,j) \simeq m_e c^2 \left[1 - \frac{\alpha^2}{2n^2} - \frac{\alpha^4}{2n^4}\left(\frac{n}{j+\frac{1}{2}} - \frac{3}{4}\right) + \ldots\right]$$

$$\rightarrow \quad hcR_\infty = \frac{1}{2} m_e \alpha^2 c^2$$

$$\alpha^2 = \frac{2R_\infty}{c}\frac{h}{m_e} \quad \Longrightarrow \quad \alpha^2 = \frac{2R_\infty}{c}\frac{A_r(\mathrm{Rb})}{A_r(\mathrm{e})}\frac{h}{m_{\mathrm{Rb}}}$$

- Hydrogen spectroscopy $\Longrightarrow$ determination of R_∞ with a relative uncertainty of 2×10^{-12}
- Determination of relative atomic masses : $A_r(X) = \frac{m_X}{m_u}$
  - Cyclotron frequencies $A_r(Rb)$ at 7.0×10^{-11}
  - Magnetic moment of a single electron bound to a carbon nucleus $A_r(e)$ at 2.9×10^{-11}

- The limiting factor is the ratio $\frac{h}{m_{Rb}}$

- G. Audi et al., 2014 Nuclear Data Sheets 120, 1-5 (2014)
- S. Sturm et al. Nature 506, 476-470 (2014),
- P. J. Mohr et al. Rev. Mod. Phys. 88, 035009 (2016).

Recoil velocity

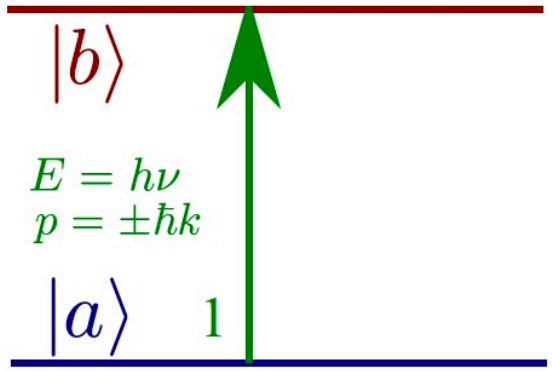

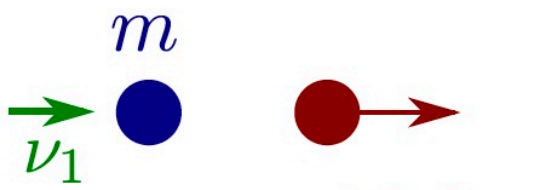

$$v_r = \hbar k/m$$

- $v_r = 6$ mm/s for *Rb* atoms
- $k = \frac{2\pi}{\lambda}$ is the wavevector and λ=780.02 nm for rubidium transition

Holger's group at Berkeley: Cs atom

R. H. Parker et al., Science 360, 191-195 (2018)

Measurement of the recoil velocity

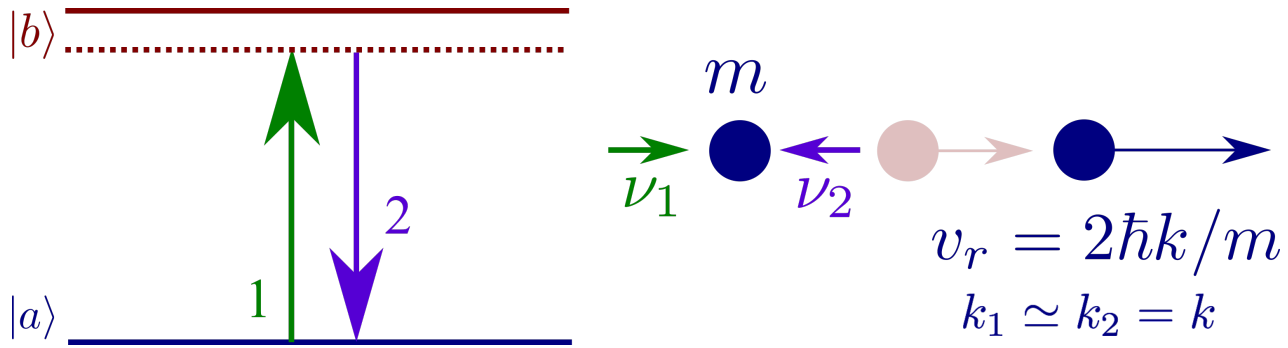

- Transfer to the atoms a large number N of photon momenta
  ⇒ Bloch oscillations technique

- Quantum velocity sensor
  ⇒ Atom interferometer based on Raman transitions with a sensitivity: σ_v

$$\sigma_{v_r} = \frac{\sigma_v}{N}$$

Coherent acceleration in optical lattice

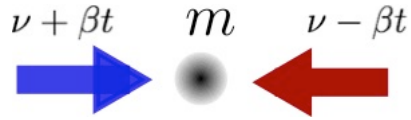

Succession of stimulated Raman transitions in the same internal level

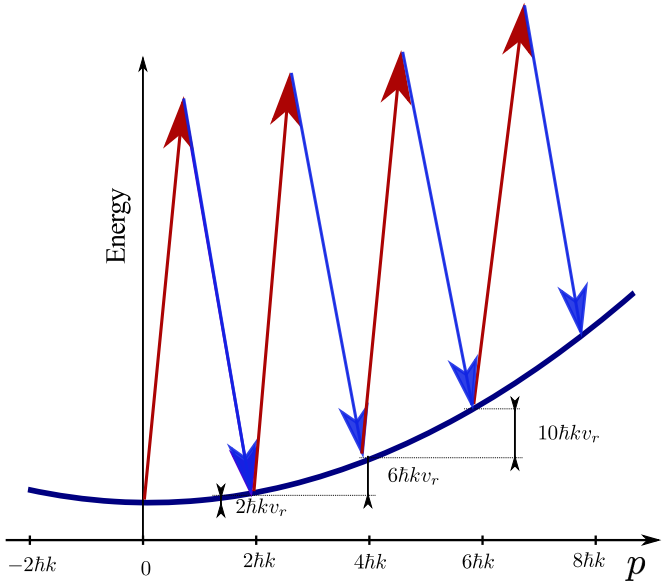

$$p_{\text{in}} \rightarrow p_{\text{in}} + 2N\hbar k$$

1000 photon momenta in 6 ms

- High momentum transfer efficiency: 99.95% per recoil
- Precise control of the velocity and the position of the atoms

Atom interferometry

Matter-light interaction

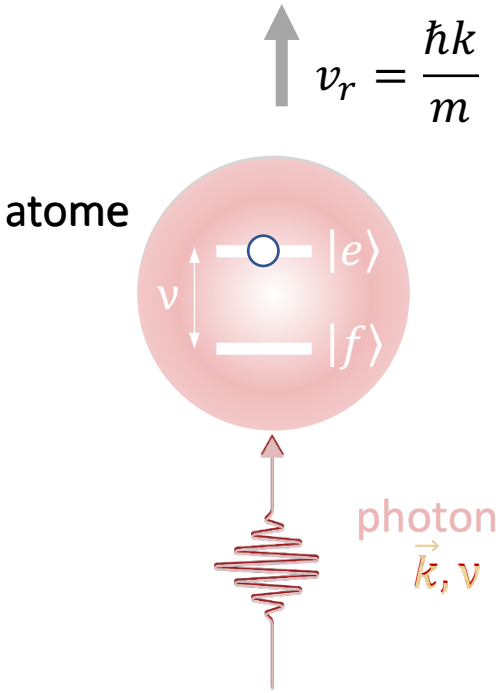

Atom interferometry

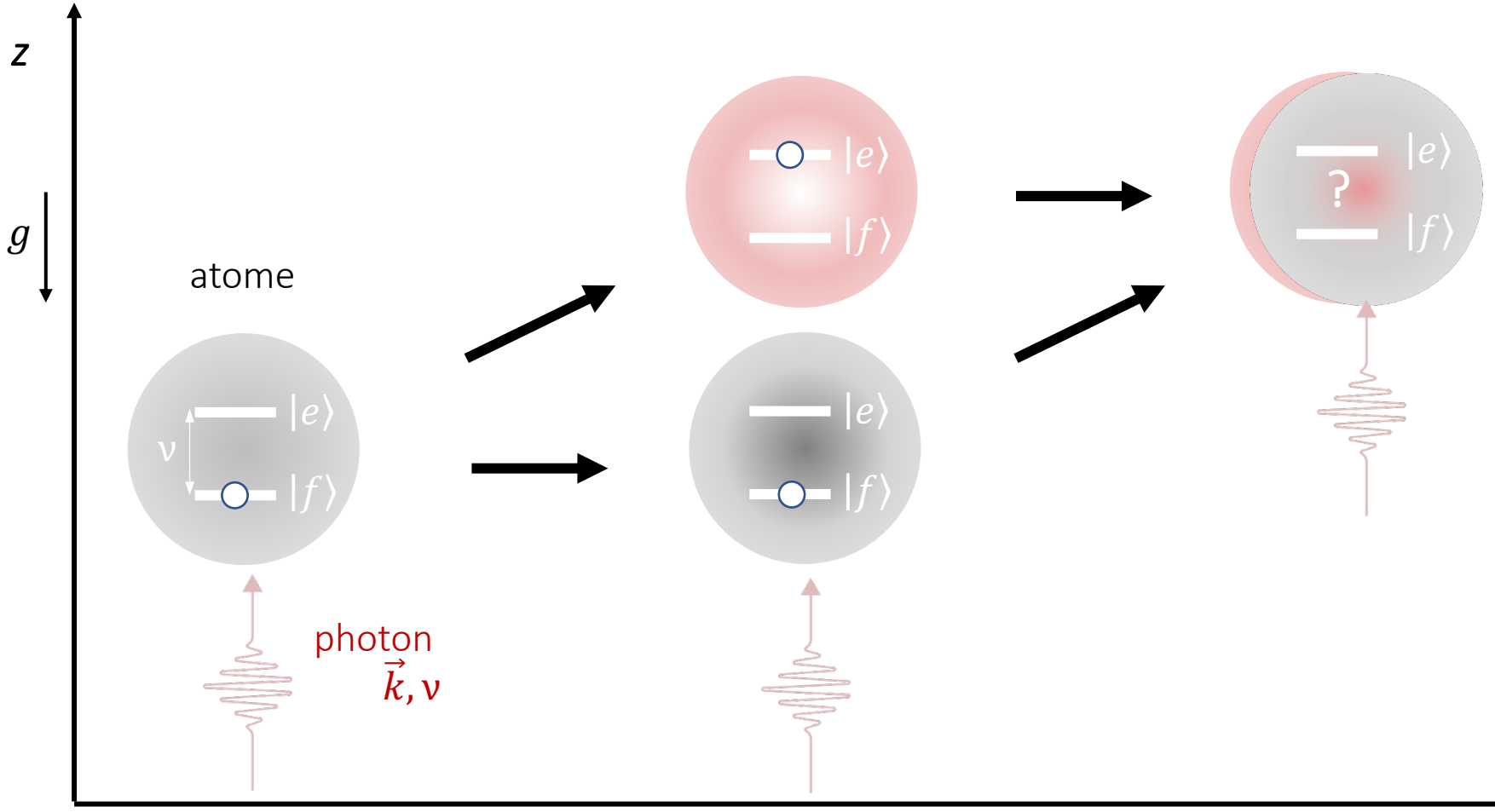

Signal :

Number of atoms in state $|e\rangle, |f\rangle$:

$$P_e = \frac{1}{2}(1 + \cos(\Delta\Phi))$$

- Atoms are sensitive to forces

Precise measurements of:

- Velocity
- Acceleration (g)
- Forces
- …

Atomic beamsplitter based on Raman transitions

$$\begin{aligned}\mathbf{E}_1(\mathbf{r},t) &= \mathbf{E}_{01}\cos(\mathbf{k}_1\cdot\mathbf{r}-\omega_{L1}t+\phi_1)\\ \mathbf{E}_2(\mathbf{r},t) &= \mathbf{E}_{02}\cos(\mathbf{k}_2\cdot\mathbf{r}-\omega_{L2}t+\phi_2)\end{aligned}$$

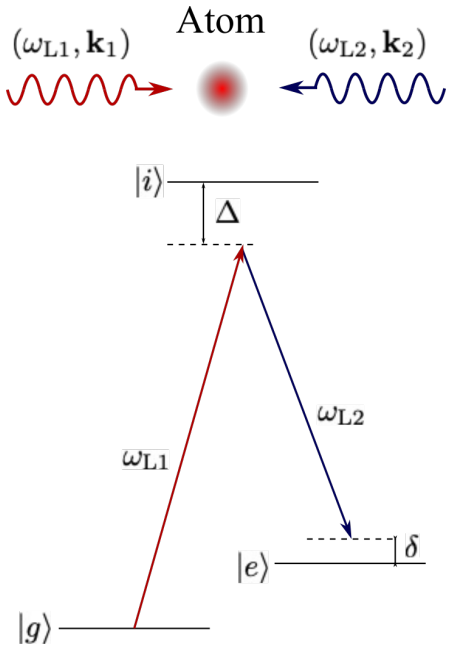

$$\Delta \gg \delta \quad \text{and} \quad \Delta \gg \Gamma$$

At resonance

$$\Psi(0) = |g,\mathbf{p}\rangle$$

$$\Psi(t) = \mathrm{e}^{-i\omega_1 t}\cos\left(\frac{\Omega_{\mathrm{eff}}t}{2}\right)|g,\mathbf{p}\rangle + \mathrm{e}^{i\Delta\phi_L}\mathrm{e}^{-i\omega_2 t}\mathrm{e}^{-i\pi/2}\sin\left(\frac{\Omega_{\mathrm{eff}}t}{2}\right)|e,\mathbf{p}+\hbar\mathbf{k}_{\mathrm{eff}}\rangle$$

$\mathbf{k}_{\mathrm{eff}} = \mathbf{k}_1 - \mathbf{k}_2$	effective wave vector
$\Delta\Phi_L$	Phase difference between the two lasers
Ω_{eff}	Effective Rabi fréquence
$\omega_1 = \omega_g + \frac{\lvert\mathbf{p}\rvert^2}{2m}$	Energy in $\lvert g,\mathbf{p}\rangle$
$\omega_2 = \omega_e + \frac{\lvert\mathbf{p}+\hbar\mathbf{k}_{\mathrm{eff}}\rvert^2}{2m}$	Energy in $\lvert e,\mathbf{p}+\hbar\mathbf{k}_{\mathrm{eff}}\rangle$

$$\Omega_{\mathrm{eff}}\tau = \frac{\pi}{2} \longrightarrow \Psi(\tau) = \frac{1}{\sqrt{2}}\left(\mathrm{e}^{-i\omega_1\tau}\,|g,\mathbf{p}\rangle + \mathrm{e}^{i\Delta\phi_L}\mathrm{e}^{-i\omega_2\tau}\mathrm{e}^{-i\pi/2}\,|e,\mathbf{p}+\hbar\mathbf{k}_{\mathrm{eff}}\rangle\right)$$

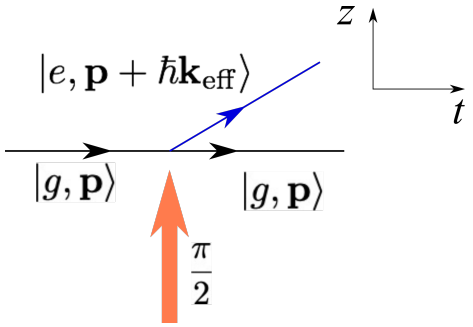

- The internal degrees of freedom are labelled by the external degrees
- Contra-propagation laser beams: velocity sensitive Raman transitions

Velocity sensor: Ramsey-Bordé Atom interferometer

Free propagation: $e^{-i\omega_{1,2}t}$, $\omega_{1,2}$, depend on the kinetic energy

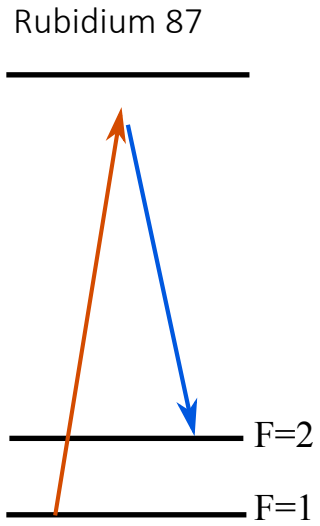

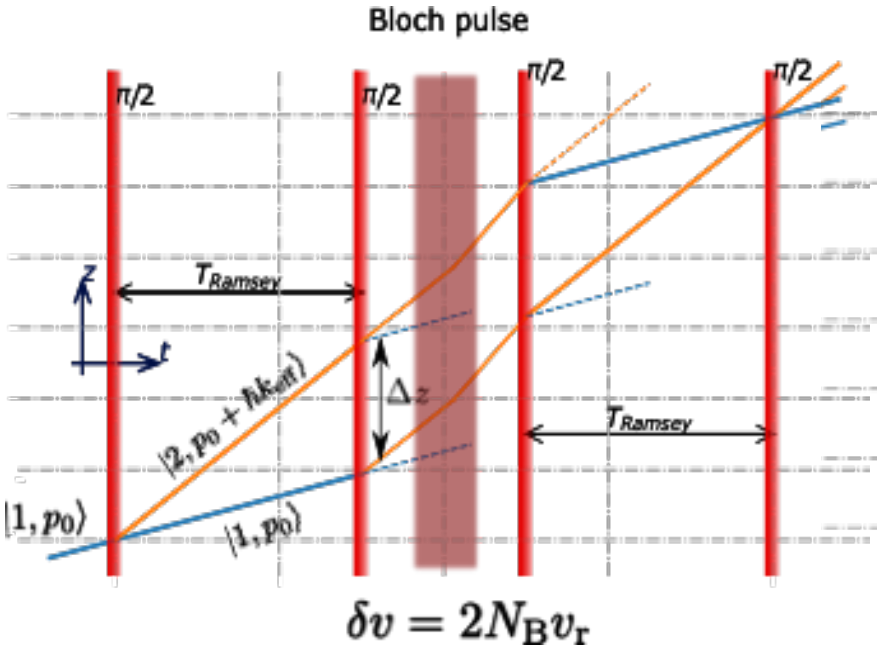

$$\delta v = 2N_B v_r$$

Probability to find an atom in $|2\rangle$

$$P_2 = \frac{1 + \cos\left(\Delta\Phi_{\text{at}} + \Delta\Phi_{\text{Las}}\right)}{2}$$

Velocity transfer δv

$$\Delta\Phi_{\text{at}} = T_{\text{Ramsey}} k_{\text{eff}} \delta v = \frac{\Delta z \times m\delta v}{\hbar}$$

Sensitivity: $\delta z = 250\ \mu\text{m} \longrightarrow 3\ \mu\text{m} \cdot \text{s}^{-1} \cdot \text{rad}^{-1}$

Interferometer for the recoil measurement

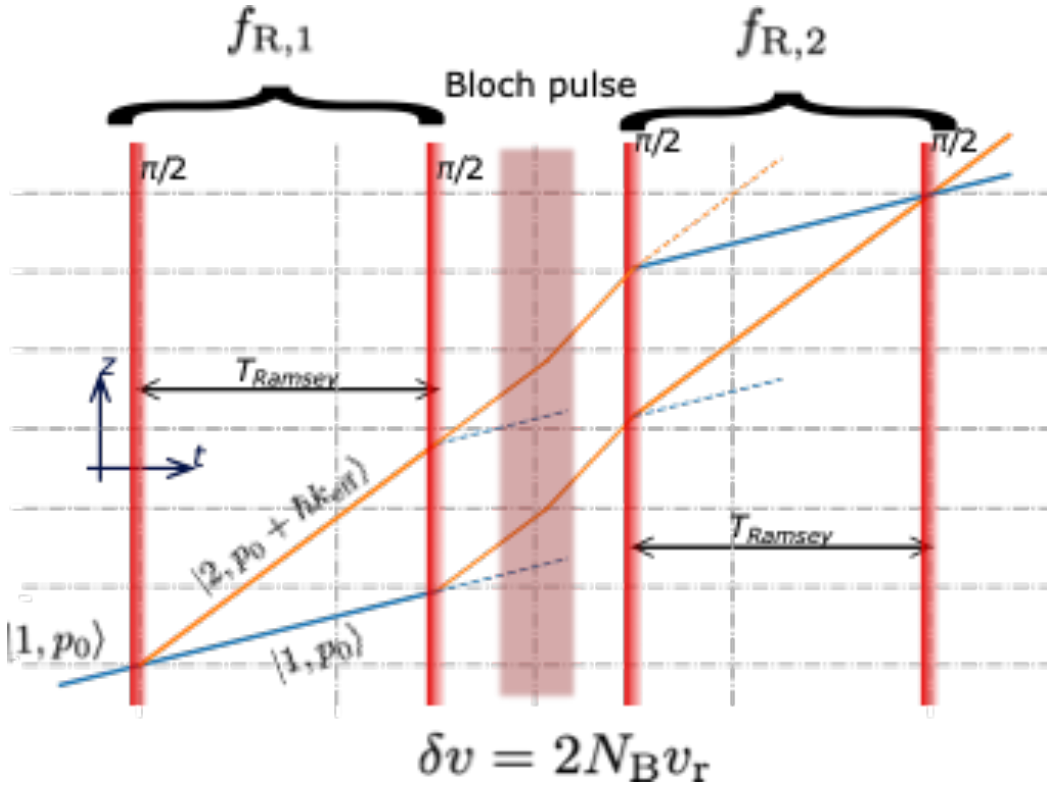

$$\delta v = 2N_{\mathrm{B}} v_{\mathrm{r}}$$

$$\Delta\Phi = T_{\mathrm{Ramsey}} \left(2N_B k_{\mathrm{R}} v_{\mathrm{r}} - 2\pi\delta f_{\mathrm{R}}\right)$$

$$\delta f_{\mathrm{R}} = f_{\mathrm{R},2} - f_{\mathrm{R},1}$$

Doppler shift

Experimental sequence

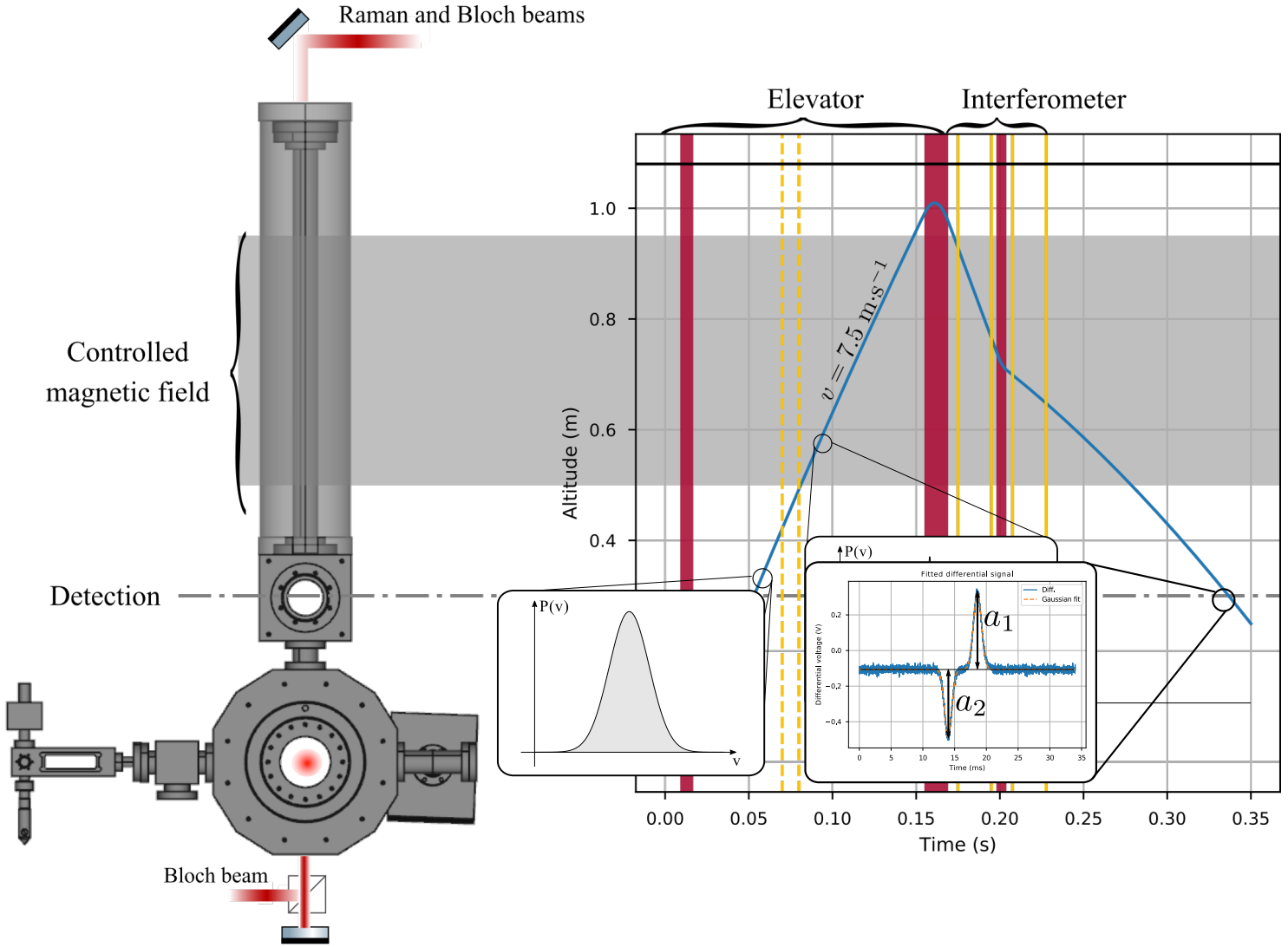

$$\begin{matrix} a_1 \propto N_1 \\ a_2 \propto N_2 \end{matrix} \longrightarrow P_2 = \frac{N2}{N_1+N_2}$$

10^8 rubidium (^{87}Rb) atoms @ T=4 μK ; radius = 600 μm

Phase and frequency control of Raman lasers

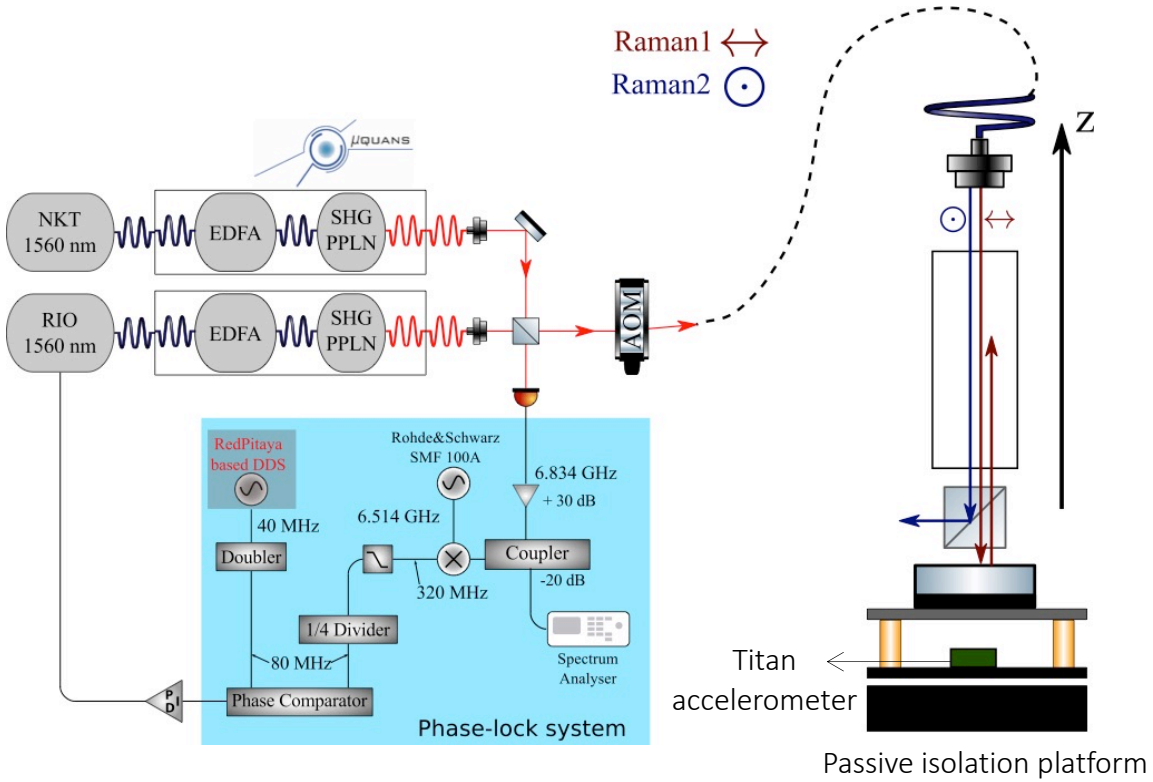

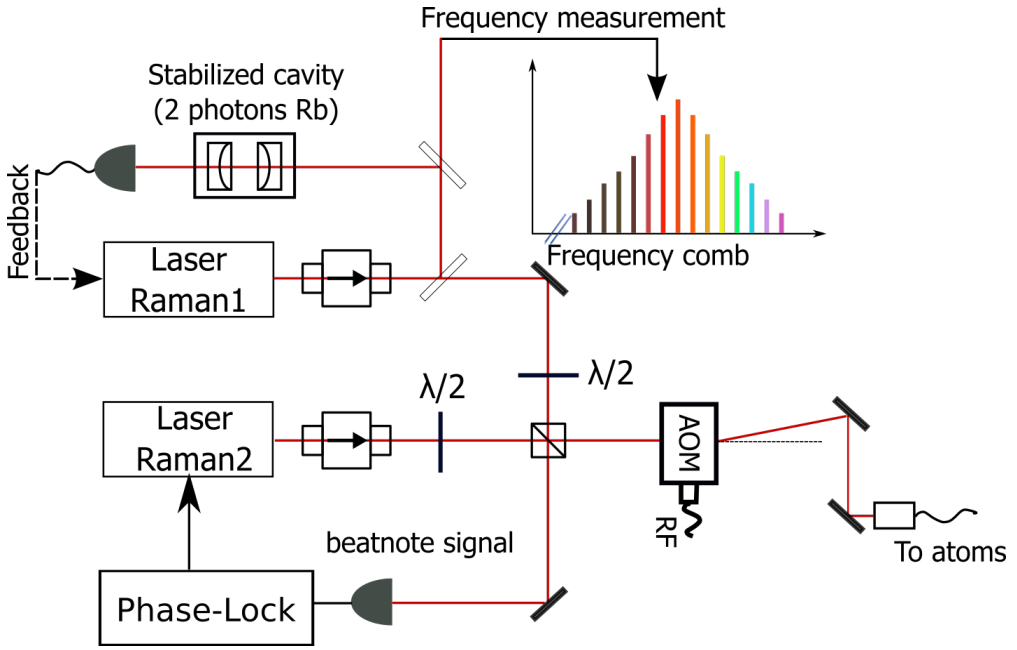

Frequency chain:

- Phase-lock of the two Raman lasers
- Frequency scanning during the second pair of $\pi/2$ pulses
- Frequency ramp to compensate for the Doppler shift during the free fall of atoms

Typical atomic fringes

- T_{Ramsey} = 20 ms, Number f Bloch oscillations N_B=500 (1000 v_r)
- 50 points per spectra in ~1 min

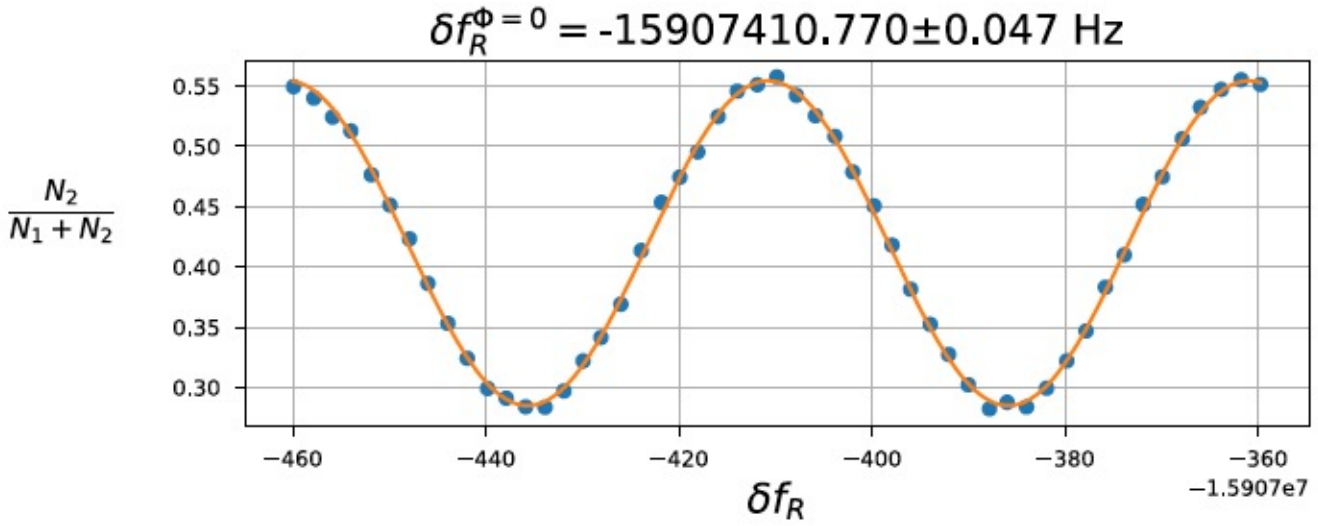

$$\Phi = T_{\text{Ramsey}}\left(k_R\left(2N_B\frac{\hbar}{m}k_B - gT\right) - 2\pi\delta f_R\right) + \Phi^{LS}$$

- Recoil velocity (one photon momentum) ~ 15 kHz → 1000 v_r ~ 15 MHz
- σ_v=4.7 mHz ~ 3 x 10^{-6} v_r ~ 20 nm s^{-1} → 3 x 10^{-9} on h/m
- Number of atoms detected=100 000 ; $\sigma_\phi = 2\sigma_{\phi SQL}$ limited by vibrations

➢ Contributions of g and the light shift Φ_{LS} cancelled using an adequate experimental protocol

Statistical uncertainty

Stable and reliable set-up: Long measurement period

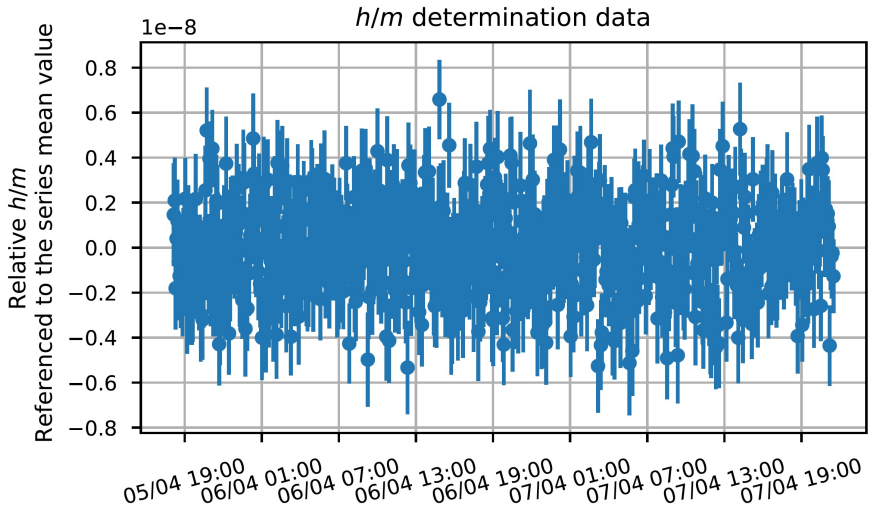

From Friday to ..... Sunday

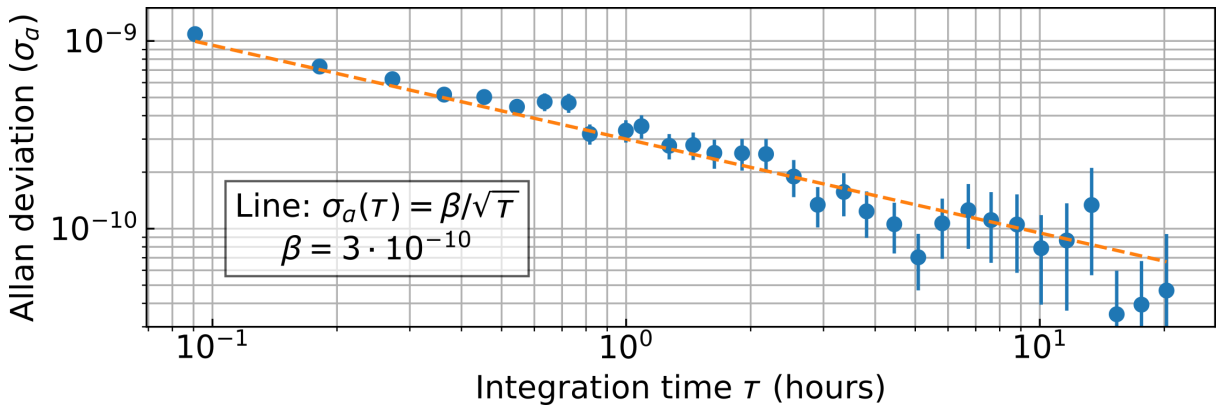

48 h integration: 8.5×10^{-11} on h/m $\longrightarrow$ 4.3×10^{-11} on α

Final data set (Jan. 2020)

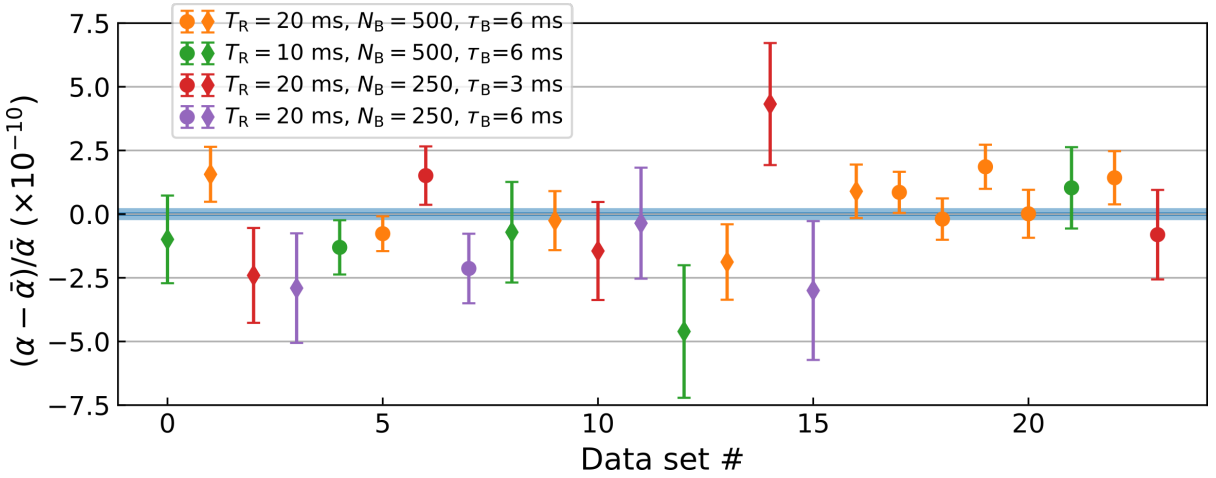

Error budget

Source	Correction $[10^{-11}]$	Relative uncertainty $[10^{-11}]$
Gravity gradient	-0.6	0.1
Alignment of the beams	0.5	0.5
Coriolis acceleration		1.2
Frequencies of the lasers		0.3
Wave front curvature	0.6	0.3
Wave front distortion	3.9	1.9
Gouy phase	108.2	5.4
Residual Raman phase shift	2.3	2.3
Index of refraction	0	< 0.1
Internal interaction	0	< 0.1
Light shift (two-photon transition)	-11.0	2.3
Second order Zeeman effect		0.1
Phase shifts in Raman phase lock loop	-39.8	0.6
Global systematic effects	64.2	6.8
Statistical uncertainty		2.4
Relative mass of ^{87}Rb [16] : $86.909\,180\,531\,0(60)$		3.5
Relative mass of the electron [14] : $5.485\,799\,090\,65(16) \cdot 10^{-4}$		1.5
Rydberg constant [14] : $10\,973\,731.568\,160(21)\mathrm{m}^{-1}$		0.1
Total: $\alpha^{-1} = 137.035\,999\,206(11)$		8.1

Atom recoil in a gaussian beam

- Electric field: $E(\vec{r},t) = A(\vec{r},t)\ \mathrm{e}^{i\phi(\vec{r})} \longrightarrow \vec{k}_{\mathrm{eff}} = \vec{\nabla}\phi(\vec{r})$
- Plane wave model: $k = \frac{\nu}{c}$
- Gaussian laser beam correction: $k_{\mathrm{eff},z} = k + \delta k$

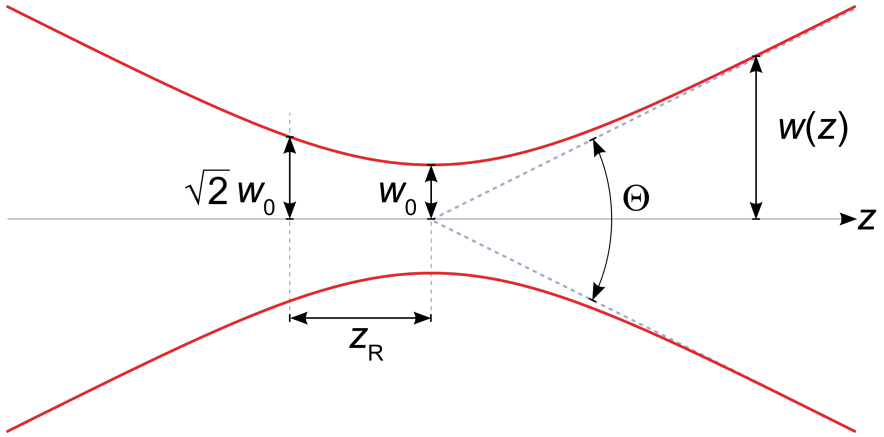

$$\frac{\delta k}{k} = -\frac{2}{k^2 w^2(z)}\left(1 - \frac{\langle r^2\rangle}{w^2(z)}\right) - \frac{\langle r^2\rangle}{2R^2(z)}$$

Size of the atomic cloud

Curvature of the wavefront

- Related to the dispersion of wavevectors $\sim \frac{\Theta^2}{2}$

Effect on α: $(108.2 \pm 5.4)\times 10^{-11}$

Recoil velocity of atom in a distorted wave front

- Electric field: $E(\vec{r},t) = A(\vec{r},t)\ \mathrm{e}^{i\phi(\vec{r})}$

$$k_{\mathrm{eff},z} = \frac{\partial\phi}{\partial z} = k + \delta k$$

Random spatial fluctuations of laser intensity with typical correlation length 100 µm

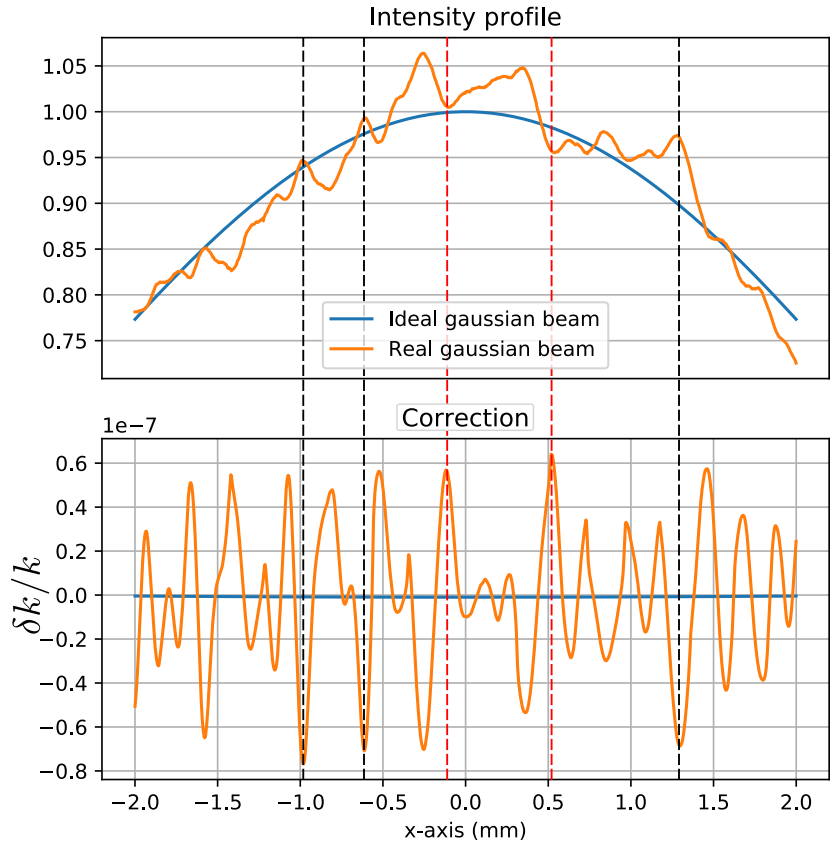

Local amplitude fluctuations induces momentum correction (in paraxial approximation)

$$\frac{\delta k}{k} = -\frac{1}{2}\left\|\frac{\vec{\nabla}_\perp\phi}{k}\right\|^2 + \frac{1}{2k^2}\frac{\triangle_\perp A}{A}$$

Correlation between the wave vector correction and the survival probability ***P*** (I) during Bloch oscillations,

$$\langle\delta k\rangle = \frac{\langle\delta k\ P(I)\rangle}{\langle P(I)\rangle}$$

S. Bade et al., Phys. Rev. Lett. **121**, 073603 (2018)

Recoil velocity of atom in a distorted wave front

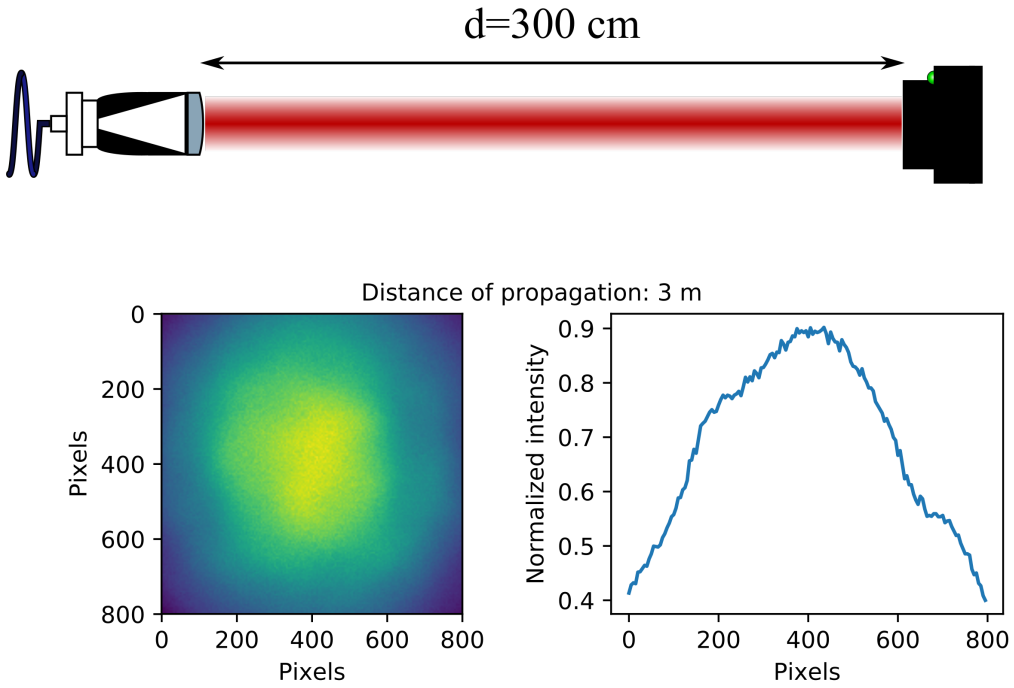

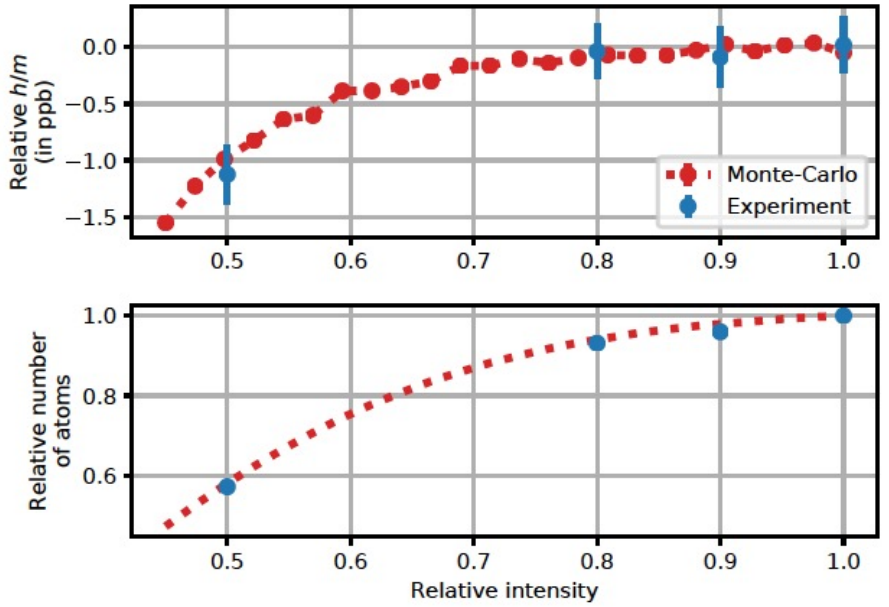

Effect on α: $(3.9 \pm 1.9)\times 10^{-11}$

Recent results

L. Morel et al., Nature 588, 61-68 (2020)

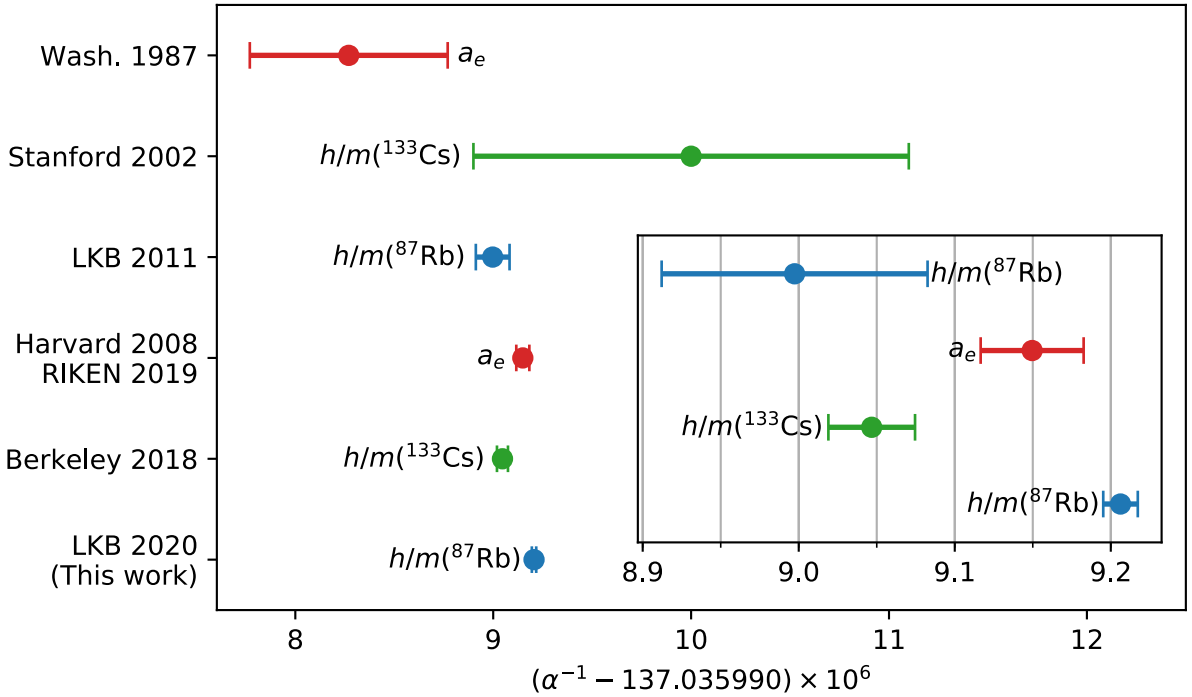

$$\alpha^{-1} = 137.035999206(11)$$

- Relative uncertainty of 8.1×10^{-11}
- Statistical uncertainty of 4.3×10^{-11} on 48 h
- New systematic effects were considered
- $5.4\ \sigma$ discrepancy with caesium recoil measurement

R. H. Parker et al., Science 360, 191-195 (2018)

New theoretical value of the electron moment anomaly

$$a_e(\mathrm{exp}) - a_e(\alpha_{\mathrm{LKB2020}}) = (+4.8 \pm 3.0) \times 10^{-13} \ (+1.6\sigma)$$
$$a_e(\mathrm{exp}) - a_e(\alpha_{\mathrm{Berkeley}}) = (-8.8 \pm 3.6) \times 10^{-13} \ (-2.6\sigma)$$

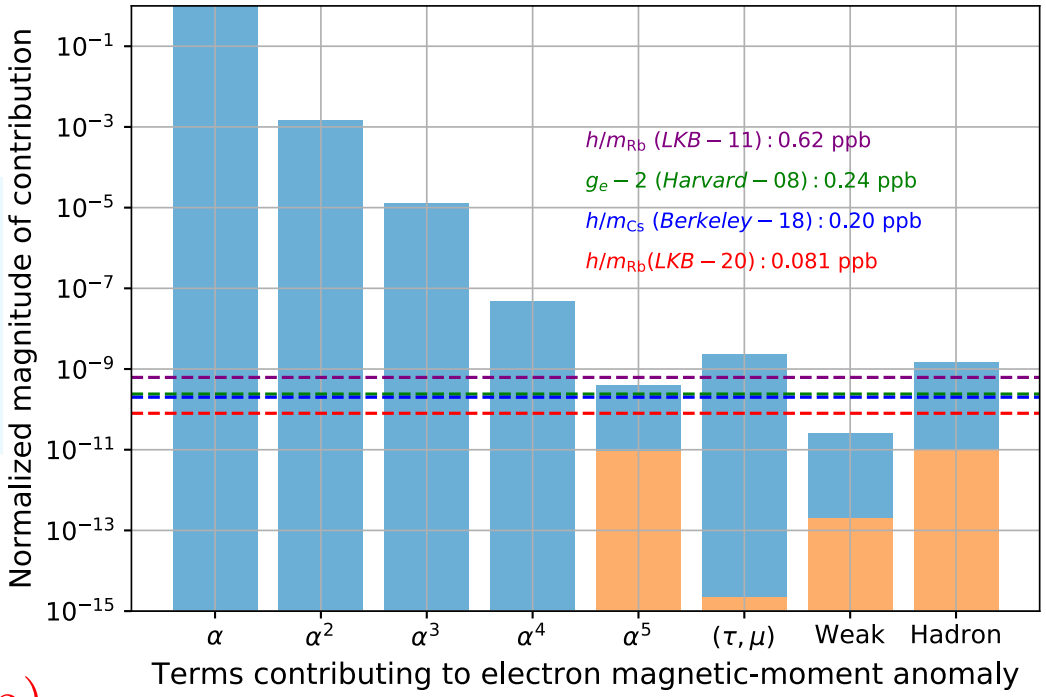

The uncertainty on δa_e is now dominated by $a_e(\mathrm{exp})$

Physics beyond Standard Model

➢ δa_e places limits on "hypothetical dark particles" parameters (coupling parameter ε and mass m_V)

Our results rejects with 95% confidence level $\delta a_e > 9.8 \times 10^{-13}$ and $\delta a_e < -3.4 \times 10^{-13}$

$$\delta a_e = \frac{\alpha}{\pi} \times \epsilon^2 \int_0^1 \mathrm{d}z \frac{2m_e^2 z(1-z)^2}{m_e^2(1-z)^2 + m_V^2 z} \simeq \frac{\alpha\epsilon^2}{3\pi} \frac{m_e^2}{m_V^2} \quad \text{For} \quad m_V \gg m_e$$

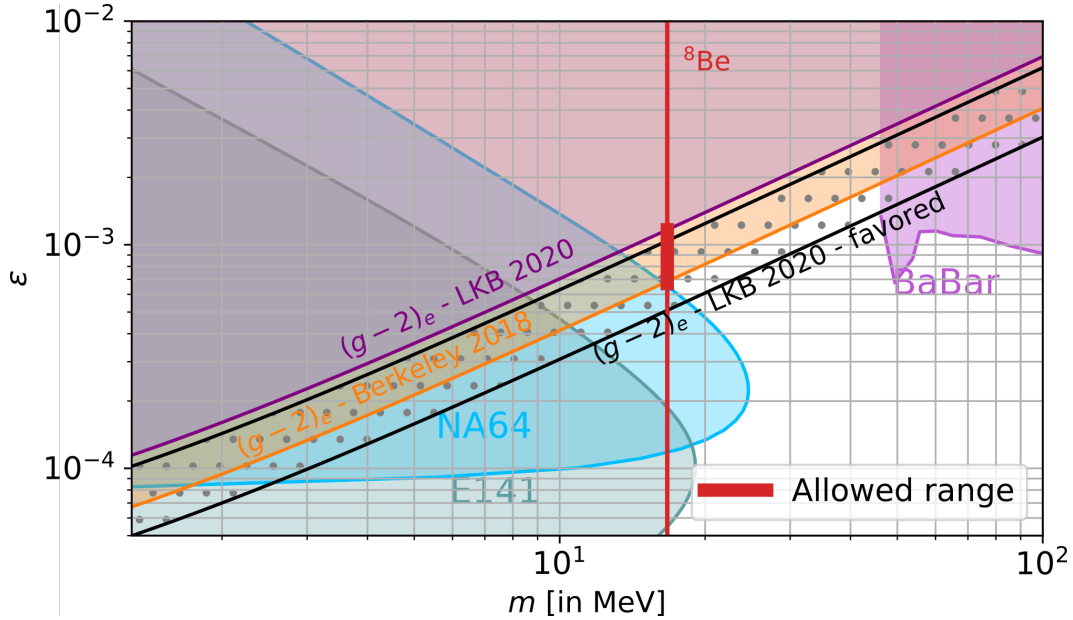

D. Banerjee et al. (The NA64 Collaboration) Phys. Rev. D 101, 071101(R) (2020)

- Favoured the hypothetical X(16.7 MeV) boson that could explain the anomalous excess of e^+e^- pairs observed in the decays of the excited ^{8}Be∗ nuclei ("Beryllium or X17 anomaly")

A. J. Krasznahorkay et al., Phys. Rev. Lett. 116, 042501 (2016)

Testing the muon a_μ discrepancy in the electron sector

- T. Aoyama et al., Physics Reports 887, 1-66 (2020)
- B. Abi *et al.* (Muon g−2 Collaboration) Phys. Rev. Lett. 126, 141801 (2021).

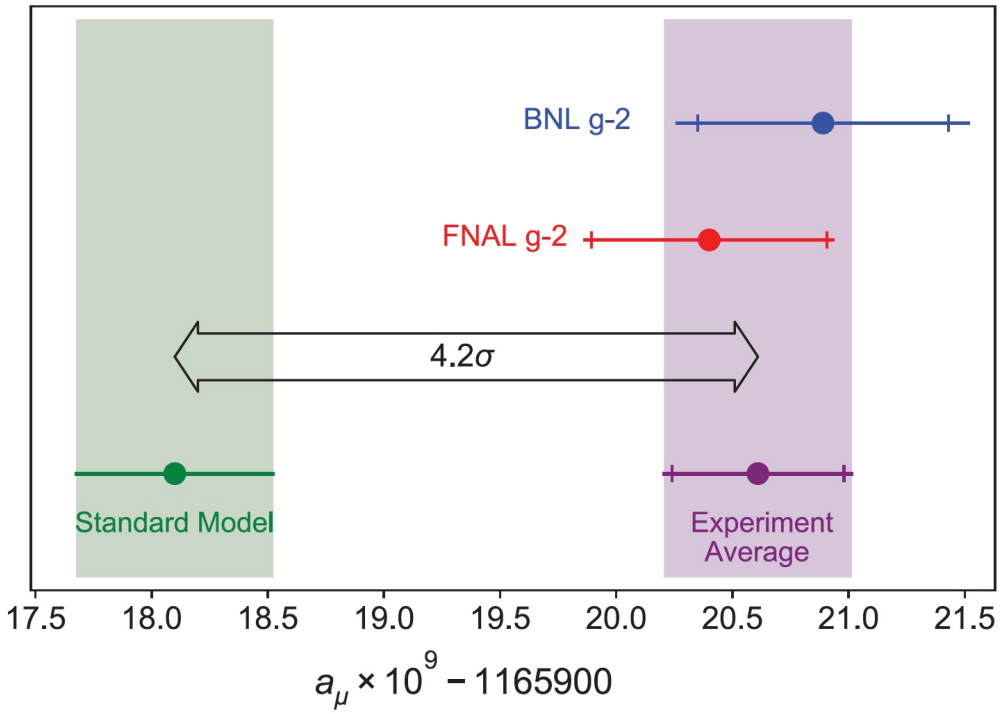

$$\delta a_\mu = a_\mu(\mathrm{Exp}) - a_\mu(\mathrm{SM}) = (251 \pm 59) \times 10^{-11}$$

$$\delta a_\mu \stackrel{?}{=} a_\mu(\mathrm{NP})$$

- Naive scaling $\left|\frac{\delta a_\mathrm{e}}{\delta a_\mu}\right| = \left(\frac{m_\mathrm{e}}{m_\mu}\right)^2 \simeq 2.3 \times 10^{-5}$

G.F. Giudice, P. Paradisi and M. Passera JHEP 11 (2012) 113,
F. Terranova and G. M. Tino, PRA 89, 052118 (2014)

$$\sigma_\mathrm{e} = 2.5 \times 10^{-5} \times \left(\frac{m_\mathrm{e}}{m_\mu}\right)^2 \simeq 5.8 \times 10^{-14}$$

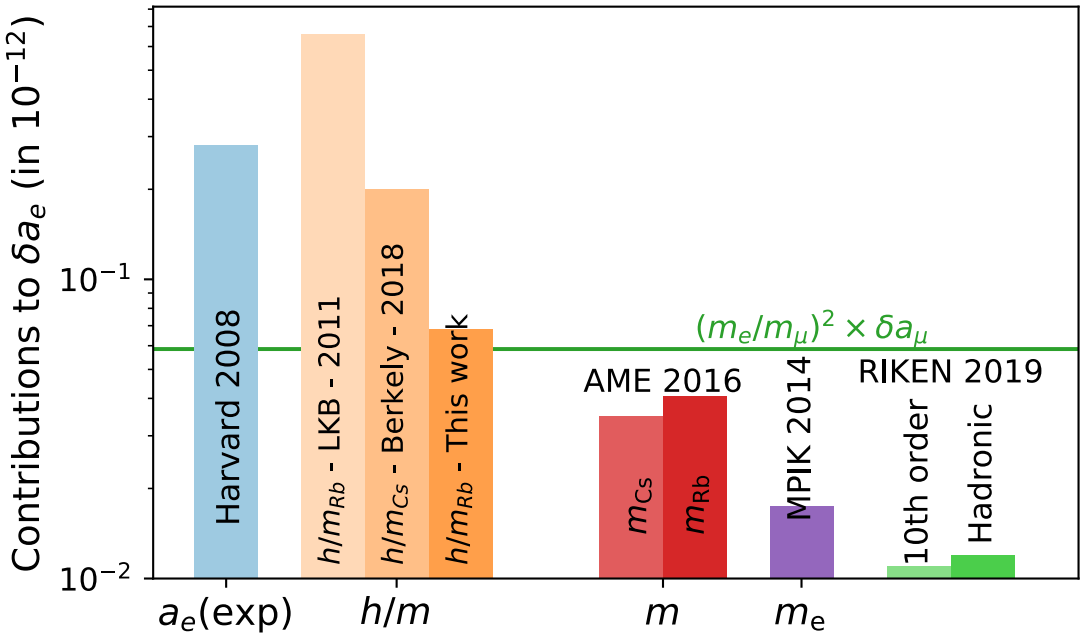

New international System of units

- The new SI (since 20 may 2019)
  Based on fundamental constants $\Delta\nu_{Cs}$, c, h, e, N_A, K_{cd}

- Our experiment allow the *Mise en pratique* of the new kilogramme at the atomic scale

$$m(^{87}\mathrm{Rb}) = 1.44316089776\ (21)\ \times 10^{-25}\ \mathrm{kg}$$

- The Avogadro constant N_A is also fixed for new definition of the mole, molar mass of carbon-12 will no longer be exactly defined

$$M(^{12}\mathrm{C}) = N_A \times m(^{12}\mathrm{C}) = \frac{12 N_A h}{h/m_\mathrm{u}} = 12.0000000173(19)\ \mathrm{g/mol} \quad \text{where} \quad m_\mathrm{u} = \frac{m_\mathrm{X}}{A_\mathrm{r}(\mathrm{X})}$$

- The fine-structure constant plays an important role in the adjustment of fundamental physical constants:
  in the new SI the numerical values of ε_0 et μ_0 will depend on a.

$$\mu_0 = \frac{2\alpha h}{e^2 c} = 0.999999999648(80) \times 4\pi \times 10^{-7}\ \mathrm{m \cdot kg \cdot s^{-2} \cdot A^{-2}}$$

90 of the 354 constants listed by NIST (https://physics.nist.gov/cuu/Constants/) will have their uncertainties reduced.

To go further

- Measurement of recoil velocity of ^{85}Rb atom
- New experimental setup : uncertainty on α of 10^{-11}
  - Larger interaction area
  - Ultra-cold atomic source
  - Larger beam waist
  - Large Momentum beam splitters in dual optical lattices.

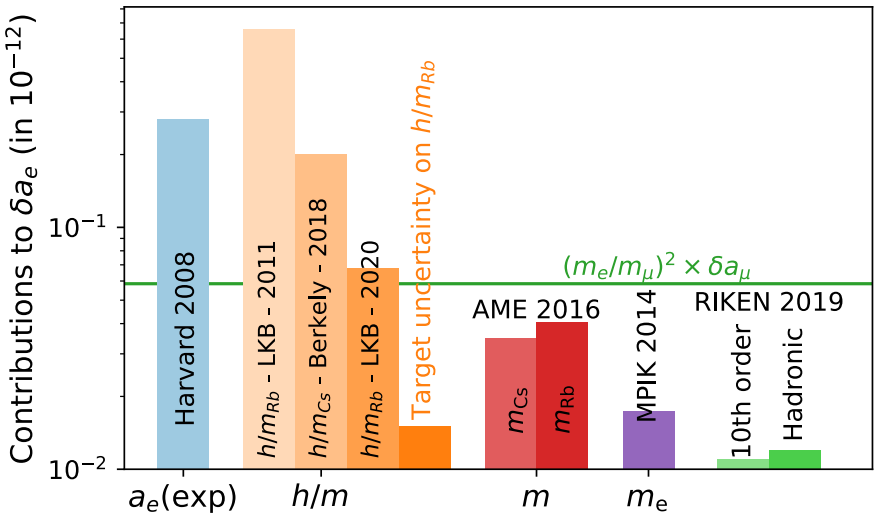

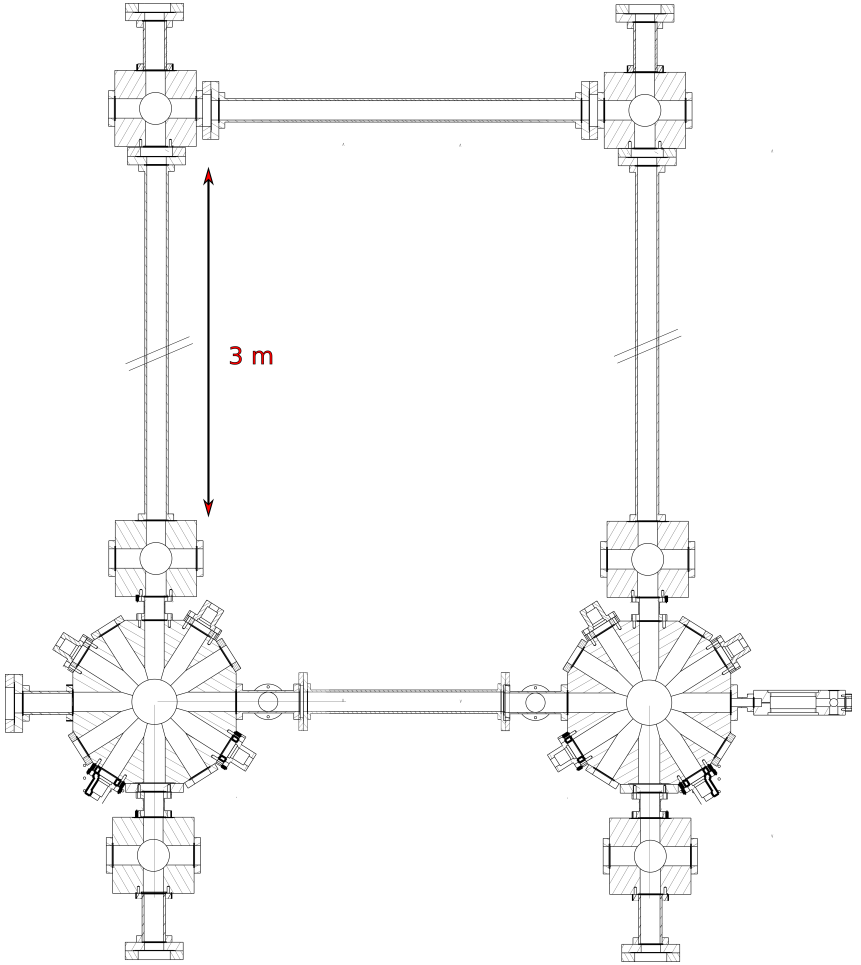

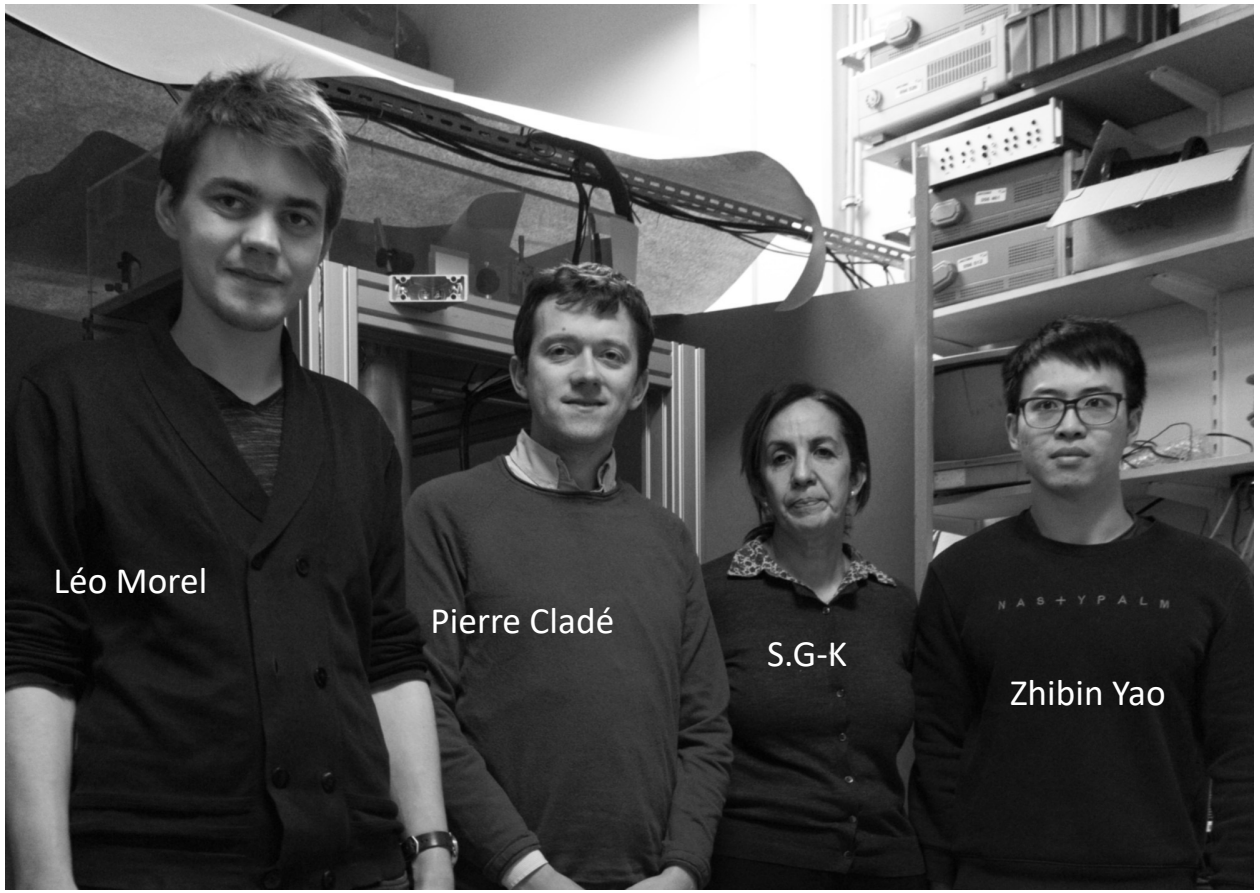

PhD students (since 2000):

- L. Morel
- Z. Yao
- M. Andia
- R. Jannin
- C. Courvoisier
- R. Bouchendira
- M. Cadoret
- P. Cladé
- R. Battesti

Thank you !

PROJET FINANCÉ PAR L'ANR - PROJECT FUNDED BY THE ANR
ANR
NIST National Institute of Standards and Technology U.S. Department of Commerce
DEPARTMENT OF JUSTICE FEDERAL BUREAU OF INVESTIGATION
DGA
Liberté • Égalité • Fraternité RÉPUBLIQUE FRANÇAISE MINISTÈRE DE LA DÉFENSE
Institut Francilien de Recherche sur les Atomes Froids
IFRAF